VEGF-A–Expressing Adipose Tissue Shows Rapid Beiging and Enhanced Survival After Transplantation and Confers IL-4–Independent Metabolic Improvements

Jiyoung Park,[1,2] Min Kim,[1,3] Kai Sun,[1,4] Yu Aaron An,[1] Xue Gu,[4] and Philipp E. Scherer[1,5]

Diabetes 2017;66:1479–1490 | https://doi.org/10.2337/db16-1081

Adipocyte-derived vascular endothelial growth factor-A (VEGF-A) plays a crucial role in angiogenesis and contributes to adipocyte function and systemic metabolism, such as insulin resistance, chronic inflammation, and beiging of subcutaneous adipose tissue. Using a doxycycline-inducible adipocyte-specific VEGF-A–overexpressing mouse model, we investigated the dynamics of local VEGF-A effects on tissue beiging of adipose tissue transplants. VEGF-A overexpression in adipocytes triggers angiogenesis. We also observed a rapid appearance of beige fat cells in subcutaneous white adipose tissue as early as 2 days postinduction of VEGF-A. In contrast to conventional cold-induced beiging, VEGF-A–induced beiging is independent of interleukin-4. We subjected metabolically healthy VEGF-A–overexpressing adipose tissue to autologous transplantation. Transfer of subcutaneous adipose tissues taken from VEGF-A–overexpressing mice into diet-induced obese mice resulted in systemic metabolic benefits, associated with improved survival of adipocytes and a concomitant reduced inflammatory response. These effects of VEGF-A are tissue autonomous, inducing white adipose tissue beiging and angiogenesis within the transplanted tissue. Our findings indicate that manipulation of adipocyte functions with a bona fide angiogenic factor, such as VEGF-A, significantly improves the survival and volume retention of fat grafts and can convey metabolically favorable properties on the recipient on the basis of beiging.

Adipose tissue in the adult organism undergoes periods of dynamic expansion and reduction under different metabolic conditions, depending on the energy needs of the host (1). To support the remodeling of adipose tissue, the plasticity of the embedded vasculature in adipose tissues is crucial to maintain appropriate access of oxygen and nutrients to the tissue (2). Although white adipose tissue (WAT) is vascularized, brown adipose tissue (BAT) is particularly highly vascularized, and the interaction between adipocytes and vascular capillaries is essential for adipocyte homeostasis under physiological and pathological conditions (1,2).

Vascular endothelial growth factor-A (VEGF-A) is classically known to be involved in vascular development during embryogenesis (vasculogenesis), as well as blood vessel formation (angiogenesis) and tissue remodeling in the adult organism (3). Recent findings highlight the roles of adipose tissue VEGF-A in the control of adipose tissue function and systemic energy metabolism through the modulation of the adipose vasculature (4,5). VEGF-A overexpression in WAT facilitates angiogenesis and thereby causes a "beiging effect" in subcutaneous WAT (sWAT), altogether resulting in a healthier expansion of WAT as well as protection against genetically and diet-induced obesity and metabolic dysfunction (4). Furthermore, VEGF-A overexpression in BAT augments vascularization and thermogenesis during chronic cold exposure and protects against systemic metabolic dysfunction induced by a high-fat

[1]Department of Internal Medicine, Touchstone Diabetes Center, University of Texas Southwestern Medical Center, Dallas, TX
[2]Department of Biological Sciences, School of Life Sciences, Ulsan National Institute of Science and Technology, Ulsan, South Korea
[3]National Research Laboratory for Mitochondrial Signaling, Department of Physiology, College of Medicine, Inje University, and Cardiovascular and Metabolic Disease Center, Inje University, Busanjin-gu, Busan, South Korea
[4]Center for Metabolic and Degenerative Diseases, The Brown Foundation Institute of Molecular Medicine for the Prevention of Human Diseases, University of Texas Health Science Center at Houston, Houston, TX
[5]Department of Cell Biology, University of Texas Southwestern Medical Center, Dallas, TX

Corresponding author: Philipp E. Scherer, philipp.scherer@utsouthwestern.edu.

Received 3 September 2016 and accepted 23 February 2017.

This article contains Supplementary Data online at http://diabetes.diabetesjournals.org/lookup/suppl/doi:10.2337/db16-1081/-/DC1.

J.P., M.K., K.S., and Y.A.A. contributed equally to this study.

diet (HFD) challenge (5). VEGF-A therefore exerts a crucial role in adipose tissue homeostasis and adaptation to altered nutrient and environmental conditions through a number of different mechanisms (2). The kinetics and extent to which the VEGF-A–induced beiging of subcutaneous fat resembles mechanistically the process induced by cold are not clear.

In the area of tissue regeneration and plastic surgery, adipose tissue is commonly used for autologous transplantation (6). However, poor survival and a high absorption rate of transplanted adipose tissue are likely caused by ischemia and insufficient adipogenic differentiation. The lack of sufficient proangiogenic activity immediately posttransplantation is the main drawback of adipose cell transplants. To overcome these issues, several attempts have been made through the modulation of the methods used to harvest the tissue, the approach used for injection, and the choice of the injection site as well as combination with adipose-derived regenerative cells, extracellular scaffolds, and embedding of angiogenic cytokines such as VEGF and epidermal growth factor (7–13). These approaches were only partially successful, and proper vascularization of implanted adipose tissue remains a big challenge. We have previously described a unique mouse model that allows us to inducibly express VEGF-A specifically in the adipocyte with very high spatial resolution (4). We examined whether VEGF-A–induced vasculature and metabolic changes in adipocytes are cell autonomous and further investigated if a metabolically healthy VEGF-A–overexpressing adipose tissue can be used for cell/tissue therapy to improve metabolic homeostasis in transplant recipients in vivo. For these studies, we used an adipose tissue–specific, doxycycline (dox)–inducible, VEGF-A–overexpressing transgenic (VEGF-Tg) mouse model (4) and used the mice as donors for fat pad implantation in normal and metabolically challenged recipients.

RESEARCH DESIGN AND METHODS

Animals

To generate a mouse model with dox-inducible VEGF-A overexpression in adipocytes, tetracycline-responsive element (TRE)–VEGF-A Tg mice were bred with adiponectin promoter–driven rtTA-Tg mice (Apn-rtTA), as previously described (4). Animals used in this study were all in a pure C57BL/6 background (The Jackson Laboratory). All experiments were conducted using littermate-controlled male mice and started when these mice were 7 weeks old. Mice were housed in cages with a 12-h dark/light cycle with free access to water and regular chow diet (5080; LabDiet, Frenchtown, NJ). For the HFD challenge experiments, mice were fed with a diet containing 60% calories from fat (D12492; Research Diets, Inc., New Brunswick, NJ). For low dosage of dox treatment in combination with HFD experiments, all mice (including controls) were fed with the HFD paste (Research Diets, Inc.) mixed with dox powder (Sigma-Aldrich) to a final concentration of 60 mg/kg. For the normal dox diet, a 600 mg/kg diet (S4107; Bio-Serv, Flemington, NJ) was used. All animal experiments were approved by the Institutional Animal Care and Research Advisory Committee at the University of Texas Southwestern Medical Center.

Fat Tissue Transplantation

Subcutaneous adipose tissues were taken from the inguinal fat pads of 7-week-old male mice. Following washing of the pads in PBS, 200-mg tissue pieces were surgically implanted into interscapular area of isogenic C57/BL6J male wild-type mice. The fat grafts were retrieved at the indicated time points for further analysis.

Quantitative PCR

Adipose tissues were harvested and homogenized in TRIzol (Invitrogen, Carlsbad, CA) using a MagNA Lyser (Roche, Basel, Switzerland) and ceramic beads. For both cell culture (stromal cells) and adipose tissue, total RNAs were lyzed in TRIzol (Invitrogen) and isolated using the RNeasy RNA extraction kit (Qiagen, Hilden, Germany) according to the manufacturer's instructions. The cDNAs were prepared by reverse transcription with 1 μg total RNA and Maloney murine leukemia virus (Invitrogen). Quantitative real-time PCRs were performed with TaqMan or SYBR gene-specific primers on an ABI Prism 7900 HT sequence detection system (Applied Biosystems, Foster City, CA). Primer sequences are listed in Supplementary Table 1. The relative amounts of all mRNAs were calculated, and GAPDH and β_2-microglobulin mRNA levels were used for the internal controls.

Histological Analysis

Tissues were fixed with 10% formalin and embedded in paraffin for histological analysis. Deparaffinized tissue slides were stained with primary antibodies for uncoupling protein-1 (UCP1) (1:200; ab23841; Abcam, Cambridge, MA), CBP/p300-interacting transactivator 1 (CITED1) (1:300; ab15096; Abcam), MAC-2 (1:500; CL8942AP; Cedarlane Laboratories), and endomucin (1:200; sc-65495; Santa Cruz Biotechnology). Biotin-labeled secondary antibodies were used. The reaction was visualized by the DAB Chromogen A system (DakoCytomation, Carpinteria, CA) and counterstained with hematoxylin. Images were acquired using a Coolscope (Nikon, Tokyo, Japan). Hematoxylin and eosin (H&E) staining and Masson's Trichrome C staining were performed by Dr. John Shelton at the University of Texas Southwestern Medical Center Histology Core.

Immunofluorescence Staining

Formalin-fixed, paraffin-embedded slides were used. Deparaffinized slides were stained with primary antibodies for MAC-2 (1:500; CL8942AP; Cedarlane Laboratories) and perilipin (20R-PP004; Fitzgerald Industries International). Fluorescence-labeled secondary antibodies were used and counterstained with DAPI. Images were acquired using the Leica confocal microscope (Leica Microsystems) and analyzed with ImageJ software (National Institutes of Health).

Systemic Metabolic Tests

Fasting glucose levels were determined after 3 h of fasting, and serum samples were collected from tail-vein blood

samples. For the oral glucose tolerance tests (OGTTs), mice were fasted for 5 h prior to administration of glucose (2.5 g/kg body weight by gastric gavage). At each of the indicated time points, serum samples were collected from tail veins. Glucose concentrations were measured using an oxidase-peroxidase assay (Sigma-Aldrich). Serum triglycerides (TGs), cholesterol (Infinity TG or cholesterol kit; Thermo Fisher Scientific, Waltham, MA), and free fatty acid (FFA) (NEFA-HR [2]; Wako Diagnostics, Tokyo, Japan) levels were measured by the kits following the manufacturer's instructions. The examination of serum adiponectin and insulin levels was done by ELISA (ALPCO, Salem, NH).

Collagen Content Assay

Tissue collagen content was measured by assessing 4-hydroxyproline levels with a kit from BioVision (Milpitas, CA). Briefly, 50 mg fat tissue was homogenized in distilled water and then mixed with 6 N HCl at 120°C for 6 h. Supernatants were dried and further incubated with chloramine-T at 25°C for 10 min, and then DMAB was added to each well and incubated at 90°C for 60 min. The absorbance was measured at 560 nm using a microplate reader as suggested by the manufacturer.

Circulating VEGF-A Measurements

Serum VEGF-A levels were measured by ELISA. Mouse whole blood was collected and serum prepared. Sera were assessed by a mouse-specific VEGF-A ELISA kit (Abcam) and analyzed according to the manufacturer's instructions.

Statistical Analysis

All results are provided as means ± SEM. All statistical analyses were performed using Prism software (GraphPad Software, La Jolla, CA). Differences between the two groups over time were determined by a two-way ANOVA for repeated measures. For comparisons between two independent groups, a Student *t* test was used. Significance was accepted as $P < 0.05$.

RESULTS

Adipocyte-Specific VEGF-A Overexpression Triggers Rapid Beiging of sWAT

Previous reports have suggested a potential role of VEGF-A in adipose tissue function and systemic energy metabolism, in part through VEGF-A's effects on stimulation of angiogenesis, macrophage M2-subtype inflammation, and BAT differentiation and its function (4). To address more directly what the kinetics of VEGF-A action on adipose tissue are, we took advantage of the high temporal resolution that our genetic approach offers. We used the adipose tissue-specific dox-inducible VEGF-A Tg mouse model. This model is a combination of two Tg mouse lines, the TRE-driven VEGF-A Tg mice (TRE-VEGF) and the adipose tissue–specific tetracycline on (Tet-on) Apn-rtTA mice. In this model, the TRE can be activated by the rtTA transcription factor in the presence of dox (4). Notably, expression of the transgene in this inducible system is strictly limited to the mature adipocyte and is not present in other cell types, such as adipogenic precursor cells and macrophages. In our previous studies, chronic overexpression of VEGF-A in adipose tissue under an HFD challenge for 8 weeks triggered beige adipose tissue-like properties in sWAT and decreased the expression of inflammatory factors such as interleukin-6 (IL-6), F4/80, and tumor necrosis factor-α in epididymal WAT (4) compared with wild-type mice. A reduction of these inflammatory markers is frequently seen in metabolically healthy adipose tissue (14,15). The new class of adipocytes observed in sWAT under these conditions is referred to as "beige" adipocytes, which emerge in sWAT and are characterized by displaying elevated levels of proteins characteristic of BAT, such as expression of UCP1 and an elevated respiratory rate (16).

To further connect elevated local VEGF-A expression to the beiging effects observed in WAT, we analyzed sWAT histologically during a time-course experiment after exposing mice to dox (Fig. 1). Histological examination of sWAT in VEGF-Tg mice revealed that within 2 days of VEGF-A exposure, widespread beiging is apparent. Smaller adipocyte size and multilocular appearance can be seen, which became even more evident at 6 days post–VEGF-A induction by H&E staining (Fig. 1*A*). We further confirmed this phenotypic change in sWAT by immunohistochemically assessing UCP1 expression and additional beige adipocyte cell markers, such as CITED1 (Fig. 1*B*, *C*, and *E*) and the endothelial cell maker endomucin. Within 2 days post–dox-diet exposure, beige adipocyte markers and endomucin are apparent in VEGF-A–expressing mice. There was very limited macrophage accumulation present in areas with pronounced beiging as determined by immunostaining with the macrophage marker MAC-2 (Fig. 1*D*). These results indicate that the rate of appearance of beige adipocytes induced by VEGF-A in sWAT occurs with rapid kinetics, within as short as 2 days after VEGF-A exposure, leading to a widespread beiging phenotype in sWAT within 6 days of induction. Importantly, although there was a transient increase in macrophage infiltration on day 2, this signal was lost as time went on. To achieve a better temporal resolution that would allow us to address the relationship of vascularization per se versus beiging, we performed an experiment within an even shorter time course. The result clearly suggests that the increased vascularization precedes the bulk of the UCP1 induction, as judged by the apparent endomucin stain that only overlaps at the 36-h time point with the emerging UCP1 stain (Fig. 1*F–I*).

VEGF-A–Induced Phenotypic Changes in sWAT Are Tissue-Autonomous Effects: Short-term Transplantation of Adipose Tissue for 1 Week

sWAT and BAT were collected after 2 days of dox exposure and assayed by Western blot analysis for UCP1 expression (Fig. 2*A*). To assess whether VEGF-A–induced phenotypic changes in sWAT are tissue autonomous, we performed adipose tissue transplantations. sWAT taken from either VEGF-Tg mice or wild-type mice given a dox

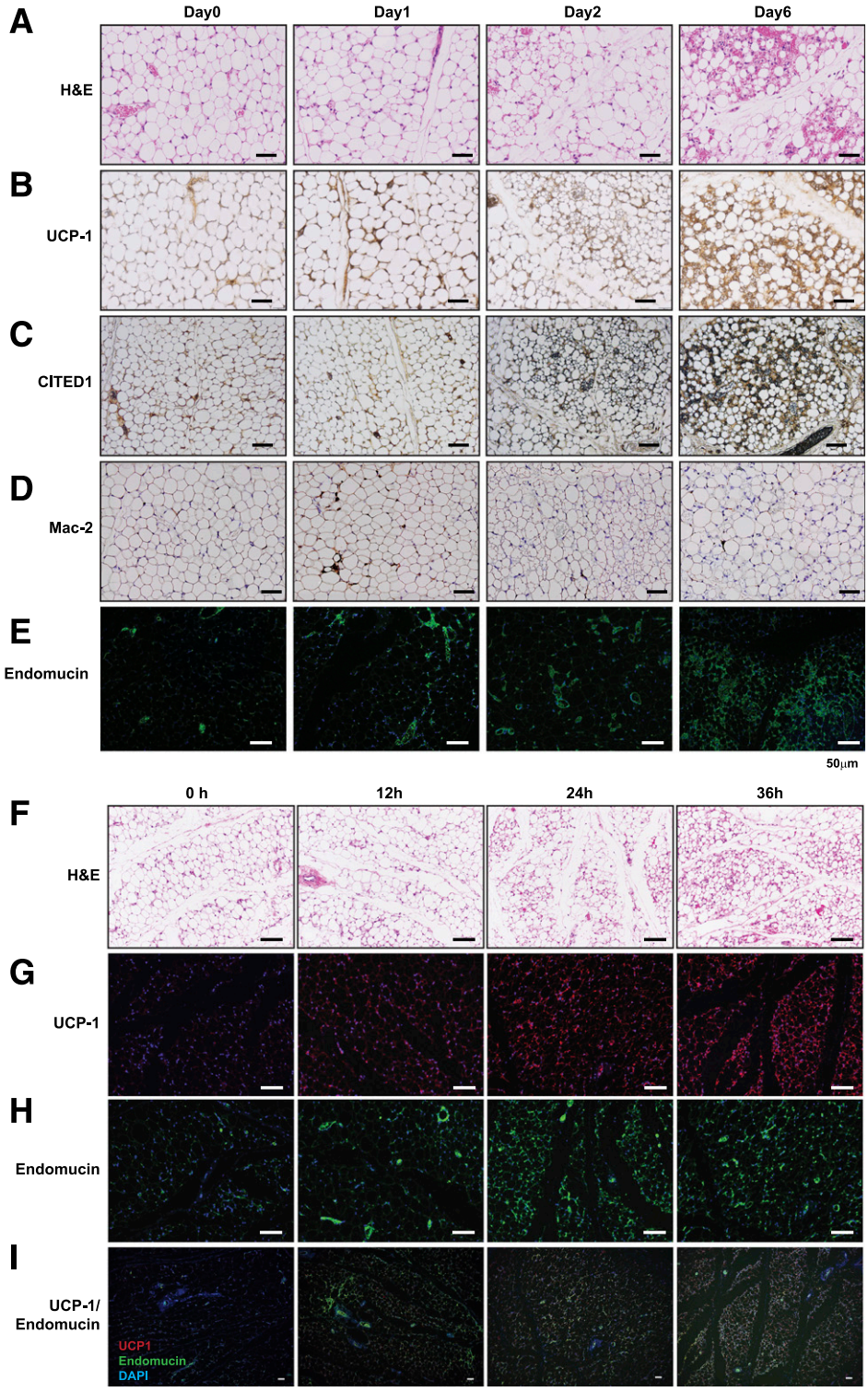

Figure 1—Time course of adipocyte-specific VEGF-A expression. VEGF-Tg mice were fed with a chow diet containing dox (60 mg/kg). At the indicated time points (days 0, 1, 2, and 6 or 0, 12, 24, and 36 h), as indicated after initiation of dox-diet feeding, mice were sacrificed, and sWAT was collected for histological analysis (n = 3 mice/each time point). *A* and *F*: H&E stain. *B* and *G*: Anti-UCP1 stain. *C*: Anti-CITED1 stain. *D*: Anti–MAC-2 stain in sWAT. *E* and *H*: Antiendomucin. *I*: Double label with endomucin and UCP1. Scale bars = 50 μm.

diet for 7 days prior to tissue harvest were subcutaneously implanted into isogenic C57/BL6J wild-type mice and maintained on a dox diet (Fig. 2*B*). Gross examination of fat grafts 7 days after implantation revealed that VEGF$^+$ sWAT grafts appeared darker in color, and more blood vessels were generated compared with control sWAT transplants (Fig. 2*B*). H&E-stained tissues also showed increased vascularization and a multilocular appearance of VEGF$^+$ sWAT

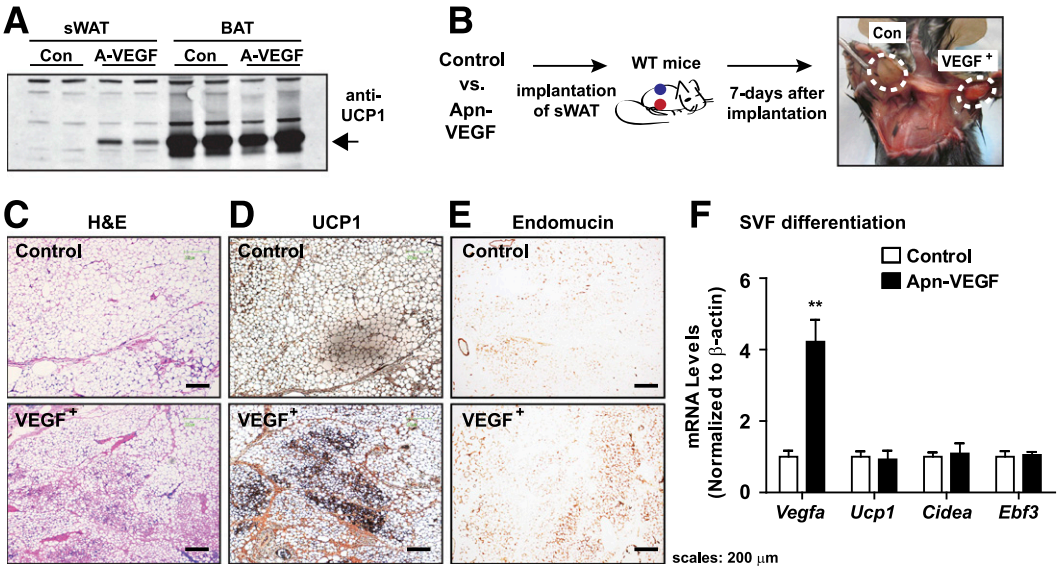

Figure 2—VEGF-A induces beiging effects in sWAT in a tissue-autonomous manner. *A*: sWAT and BAT were collected after 2 days of dox exposure and assayed by Western blot analysis for UCP1 expression. A-VEGF, Apn-VEGF. *B*: Schematic diagram of sWAT transplants. VEGF-Tg and wild-type mice were fed with a chow diet containing dox (60 mg/kg) for 7 days. sWAT donor tissues were harvested from either wild-type or VEGF-Tg mice and subcutaneously implanted into left flank (sWAT from wild-type mice [Control]) and right side (sWAT from VEGF-Tg mice [VEGF$^+$ sWAT]) of intrascapular area of isogenic C57/BL6J male mice (n = 3). Recipient mice were exposed to a chow diet containing dox (60 mg/kg) for 7 days. Fat transplants from recipient mice were harvested and examined by histological analysis. H&E staining (*C*), anti-UCP1 staining (*D*), and antiendomucin staining (*E*) were performed for VEGF-A$^+$ fat grafts and compared with control fat transplants. Scale bars = 200 μm. *F*: Stromal vascular cells (SVF) were harvested from the donors, in vitro differentiated into adipocytes, and induced with dox. Quantitative PCR analysis was performed on *Vegfa*, *Ucp1*, *Cidea*, and *Ebf3*. $^{**}P < 0.01$. All data are presented as mean ± SEM.

compared with control tissues (Fig. 2*C*). Immunostaining for UCP1 confirmed that BAT-like phenotypic changes in VEGF$^+$ sWAT grafts were still intact in the setting of 7 days after implantation (Fig. 2*D*). Furthermore, the Tg transplants were significantly better vascularized, as judged by the much denser endomucin stain seen in the transplanted fat pads expressing VEGF-A (Fig. 2*E*). These results indicate that VEGF-A–induced phenotypic changes in sWAT reflect tissue-autonomous effects, and these are sustained for at least 1 week postimplantation.

However, if stromal vascular cells are harvested from the donor and in vitro–differentiated into adipocytes, there is no difference with respect to the induction of any of the beige marker genes in the continued presence of VEGF-A induction during differentiation in vitro (Fig. 2*F*), indicating that the effects are not adipocyte autonomous, consistent with our previous report demonstrating that in vitro treatment of mature adipocytes with exogenous VEGF-A did not result in an induction of a beiging program (17).

VEGF$^+$ sWAT Grafts Can Convey Systemic Metabolic Improvements to the Host After Prolonged Transplant

In our previous study, we found that VEGF-A overexpression in sWAT ameliorates hypoxia, fibrosis, and proinflammatory responses induced by an HFD challenge (4). To test whether exogenously implanted VEGF-A$^+$ fat tissues can contribute to systemic metabolism of HFD-challenged host mice, either control or VEGF-A$^+$ sWAT pads were taken from wild-type or VEGF-Tg mice 1 week after dox-diet exposure, respectively, and subsequently implanted into isogenic wild-type mice. Following sWAT implantation, these mice were fed with an HFD combined with dox for 3 weeks (Fig. 3*A*). Fasting glucose levels in circulation were not significantly different in VEGF-A$^+$ fat–implanted mice compared with control fat–implanted mice at the end of this period (Fig. 3*B*). Body weight changes were also comparable in both groups (data not shown). To provide an additional carbohydrate challenge, we performed OGTTs on mice carrying for VEGF-A$^+$ or wild-type fat implants. Mice carrying VEGF-A$^+$ fat transplants showed enhanced glucose tolerance compared with mice receiving control transplants (Fig. 3*B*). VEGF-A–expressing transplanted fat pads can therefore exert a significant positive impact on metabolic homeostasis of recipient mice. Extracts of the transplanted fat pads were analyzed at the end of the study period for a number of parameters. There were significantly higher levels of VEGF-A mRNA seen in the Tg versus wild-type fat transplants (Fig. 3*C*). As expected, higher *Ucp1* mRNA levels were observed in the VEGF$^+$ transplants (Fig. 3*D*). VEGF-A action also translated into the expected higher vascular density as judged by the higher levels of *Cd31* mRNA (Fig. 3*E*). There were significant lower levels of inflammatory markers found in the VEGF-A$^+$ fat pads. Reduced F4/80 levels along with reduced serum amyloid A3 and lower tumor necrosis factor-α mRNA were observed, whereas *Il6* levels seemed unchanged (Fig. 3*F*). These reduced inflammatory markers reflect an overall

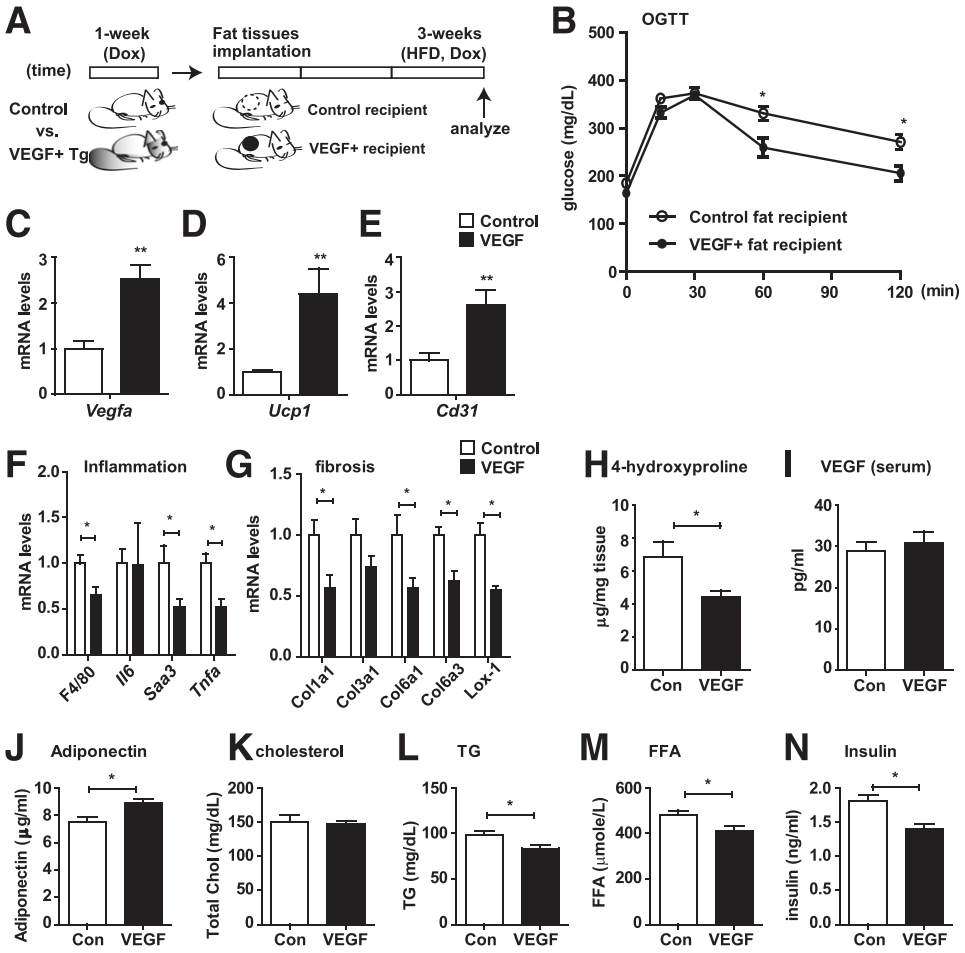

Figure 3—VEGF$^+$ fat transplants improve glucose tolerance upon an HFD challenge. *A*: Schematic diagram of sWAT transplantation. Wild-type controls and VEGF-Tg mice were fed with a chow diet containing dox (60 mg/ kg) for 1 week. sWAT from either control mice or mice expressing VEGF$^+$ was harvested and subsequently implanted into C57/BL6J wild-type hosts. The recipient mice were fed with an HFD containing a low dose of dox (60 mg/ kg) for 3 weeks. *B*: Glucose levels were determined during an OGTT 3 weeks posttransplantion after continued HFD feeding. The difference at each time point was analyzed by Student *t* test. $^*P < 0.05$ (n = 5/group). All data are represented as mean ± SEM. Transplanted adipose tissues were harvested after 3 weeks, and quantitative PCR (qPCR) analysis was performed for VEGF-A (*C*), UCP1 (*D*), and CD31 (*E*). *F*: Inflammatory markers were analyzed by qPCR. *G*: Fibrosis markers were analyzed by qPCR. Results were analyzed by Student *t* test. $^*P < 0.05$, $^{**}P < 0.01$ vs. control (n = 5/group). *H*: 4-Hydroxyproline levels of adipose tissue implants. *I*: Serum VEGF-A levels. *J*: Adiponectin. *K*: Cholesterol. *L*: TGs. *M*. FFAs. *N*: Insulin. $^*P < 0.05$. All data are presented as mean ± SEM.

healthier fat pad, and consistent with these improvements, there is significantly less fibrosis seen in the VEGF-A$^+$ fat pad, as judged by gene expression of extracellular matrix proteins and total collagen levels in the transplanted tissue (Fig. 3*G* and *H*). To address systemic effects of transplantation with VEGF-A$^+$ fat tissue, we measured serum VEGF-A levels of the host animals. The effects of VEGF-A production in the transplanted fat pads seem to be restricted to the local microenvironment, as there is no significant difference in circulating VEGF-A levels compared with mice receiving wild-type transplants (Fig. 3*I*). In addition, there was no evidence suggesting that the transplantation of VEGF-A$^+$ fat pads led to beiging of WAT of the host (Supplementary Fig. 1). The VEGF-A$^+$ fat transplants led to significant improvements in systemic parameters as well, beyond the improvements in the OGTT. Adiponectin levels were increased in circulation (Fig. 3*J*). Although circulating cholesterol levels were unaffected, significant improvements in circulating TGs, nonesterified FFAs, and insulin were observed (Fig. 3*K*–*N*).

VEGF-A Overexpression in Adipocytes Promotes Cell Survival and Functionality in Transplants

A qualitative histological examination of fat grafts after the HFD challenge revealed that VEGF-A$^+$ fat grafts are histologically quite distinct from control transplants (Fig. 4*A*). Enhanced vascularization was further confirmed with endothelial markers, such as an antiendomucin stain (Fig. 4*B*). UCP1 staining for VEGF$^+$ fat grafts further reflects extensive browning of sWAT compared with control (Fig. 4*C*). These results revealed that VEGF-A–induced angiogenesis and beiging effects in sWAT remain intact in fat grafts even 3 weeks after implantation.

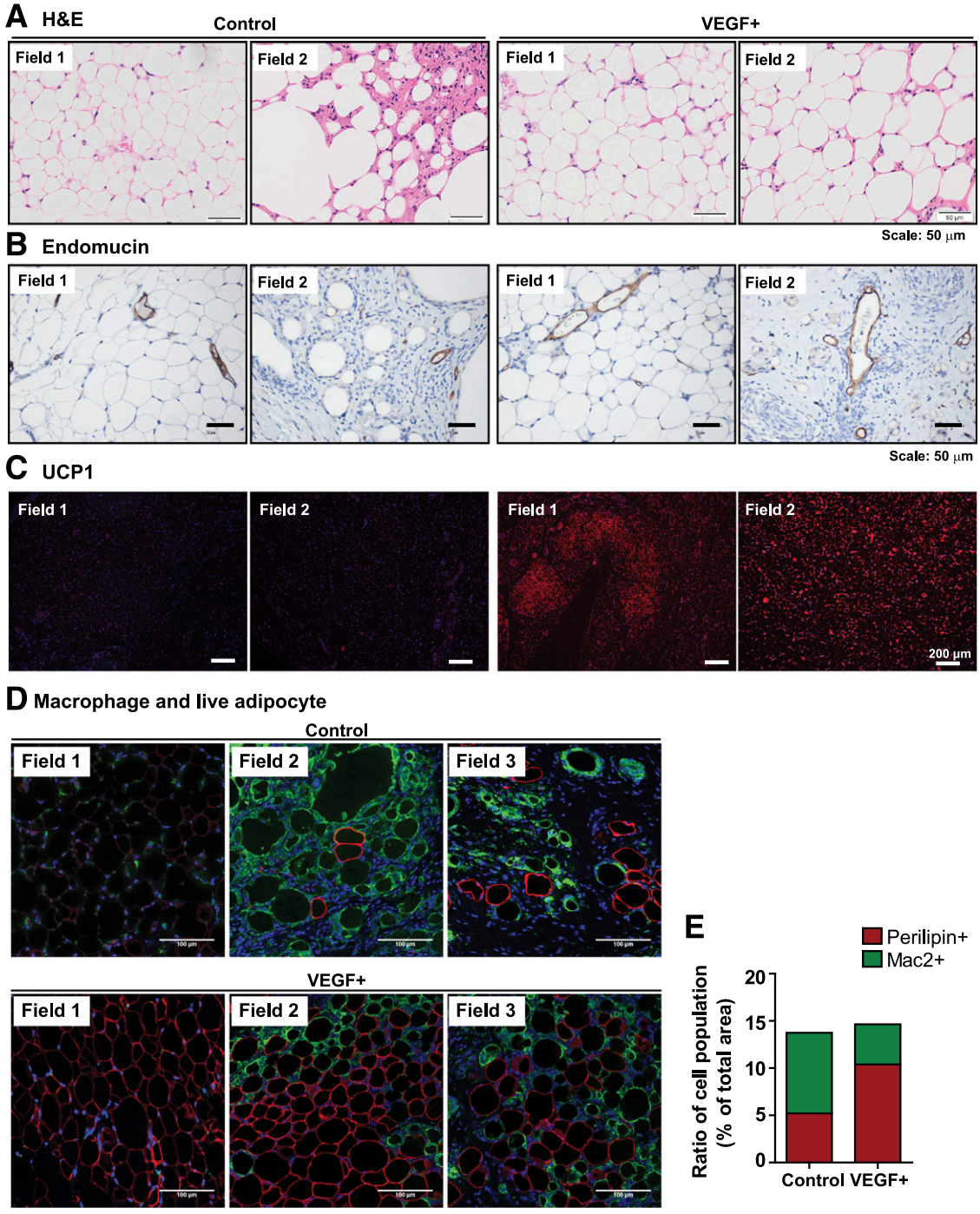

Figure 4—The survival rate of adipocytes in VEGF$^+$ fat grafts is increased compared with wild-type fat transplants. Control and VEGF-A$^+$ fat implants were taken from the host 3 weeks after the HFD challenge containing a low dose of dox (60 mg/kg). sWAT fat grafts from both groups (wild type, left panels; Tg, right panels) were subjected to histological analysis (n = 5/group). Two representative fields are shown for each condition. *A*: H&E stain. Scale bars = 50 μm. *B*: Antiendomucin stain. Scale bars = 50 μm. *C*: Anti-UCP1 stain. Scale bars = 200 μm. *D*: Immunofluorescence stain for MAC-2 (macrophage marker, green) and perilipin (live adipocyte marker, red). Costain with DAPI (nuclei, blue). Scale bars = 100 μm. Wild-type controls in top panel; Tg in the bottom panel. *E*: The ratio of perilipin$^+$ and MAC-2$^+$ cell populations was calculated.

Adipose vasculature and beiging effects are associated with metabolic benefits to adipose tissues. To see if these properties confer better survival posttransplantation, VEGF-A$^+$ fat grafts were stained with the adipocyte marker perilipin (Fig. 4*D*, red). Only live adipocytes retain a perilipin-positive stain on their lipid droplets. The macrophage marker MAC-2 was used in parallel to monitor the degree of local inflammation (Fig. 4*D*, green). The survival rate of adipocytes was dramatically increased in VEGF-A$^+$ fat grafts with reduced macrophage infiltration relative to

control fat grafts (Fig. 4*D* and *E*). These results suggest that VEGF-A overexpression in adipocyte increases the survival of adipocytes in fat grafts, thereby explaining the reduced levels of inflammatory markers as well as the reduced fibrotic response seen in Fig. 3.

VEGF-A Overexpression in Adipocytes Promotes Beiging in an IL-4– and Adiponectin-Independent Manner

Previous work suggested that both adiponectin and IL-4 are important components in the context of beiging of sWAT. Adiponectin overexpression leads to enhanced levels of beiging (18,19), whereas cold-induced beiging and browning were postulated to involve IL-4. Genetic loss of IL-4 signaling impairs cold-induced biogenesis of beige fat (20). We wanted to test whether the VEGF-A–induced beiging process has similar requirements as the cold-induced beiging, or whether we can highlight mechanistic differences. We were therefore breeding the adipocyte-specific inducible VEGF-A mice into the IL-4– and adiponectin-null backgrounds. Histologically, it did not make a difference whether the VEGF-A induction was done in a wild type (not shown), an IL-4–heterozygous state, or in an IL-4–null background (Fig. 5*A*). Comparable areas of UCP1 induction were seen independent of IL-4 genotype (Fig. 5*B*). We confirmed that IL-4 is indeed absent in the IL-4–null background (Fig. 5*C*), whereas the degrees of *Ucp1* mRNA induction were comparable even in the IL-4–null background (Fig. 5*D*). Similarly, the beiging process was completely independent of the presence or absence of adiponectin (Fig. 5*E–H*). When we tested the requirement of IL-4 for cold-induced beiging, we saw indeed that both BAT and sWAT were visibly less "dark," potentially reflecting reduced induction of the mitochondrial program (Fig. 6*A*). Post–cold exposure, the entire beiging and browning program in BAT was reduced (Fig. 6*B* and *C*), and this was further confirmed histologically by H&E stains and anti-UCP1 immunostains (Fig. 6*D–F*), confirming in our hands the previously established findings that the process of beiging and browning critically relies on IL-4.

The Beiging Effect in sWAT Is Rapidly Lost After VEGF-A Elimination

We exposed wild-type and VEGF-A Tg mice to dox for 3 days to fully induce the beiging program. We then

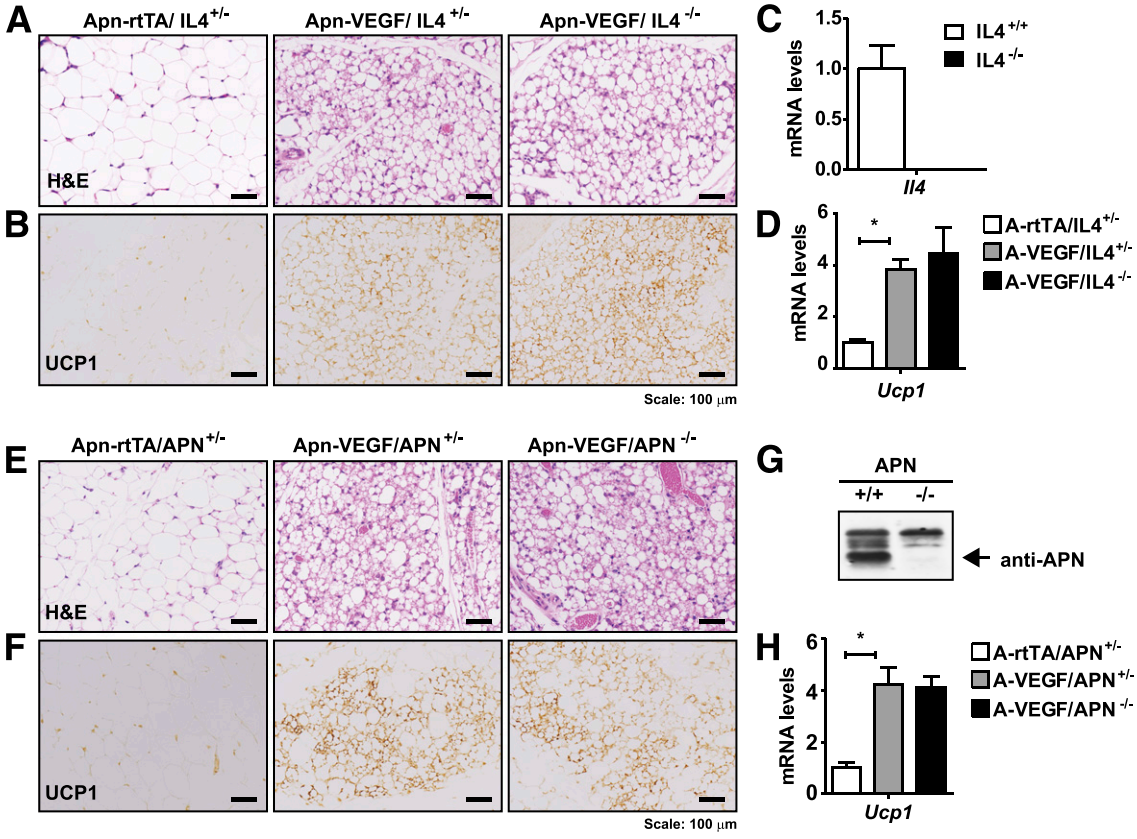

Figure 5—The VEGF-A–induced beiging is IL-4 and adiponectin independent. *A*: H&E stain of IL-$4^{+/-}$ mice carrying only the Apn-rtTA transgene (left panel), mice carrying the full Apn-rtTA × TRE-VEGF-A complement in the IL-$4^{+/-}$ background (middle panel), or Apn-rtTA × TRE-VEGF-A complement in the IL-$4^{-/-}$ background (right panel) after dox induction for 4 days. *B*: The same panels stained for UCP1. *C*: IL-4 is indeed absent in the spleens of IL-4–null mice. *D*: Quantitative PCR (qPCR) analysis of sWAT for *Ucp1* expression in the different IL-4 genetic backgrounds. A, Apn. *E*: H&E stain of adiponectin (APN)$^{+/-}$ mice carrying only the Apn-rtTA transgene (left panel), mice carrying the full Apn-rtTA × TRE-VEGF-A complement in the $APN^{+/-}$ background (middle panel), or Apn-rtTA × TRE–VEGF-A complement in the $APN^{-/-}$ background (right panel) after dox induction for 4 days. *F*: The same panels stained for UCP1. *G*: APN is indeed absent in the serum of adiponectin-null mice. *H*: qPCR analysis of sWAT for *Ucp1* expression in the different APN backgrounds. Scale bars = 100 μm. *$P < 0.05$. All data are presented as mean ± SEM.

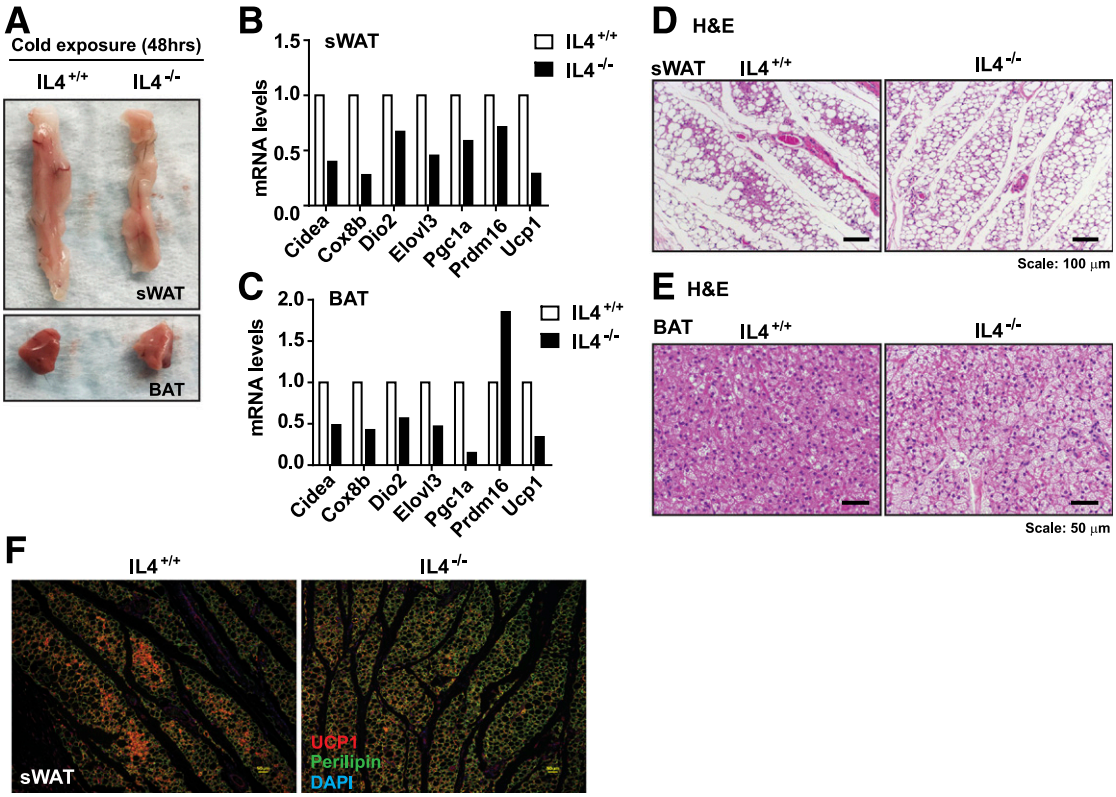

Figure 6—Systemic lack of IL-4 leads to impaired cold-induced beiging. *A*: Overall appearance of excised sWAT (top) and BAT (bottom) in either wild-type (IL-$4^{+/+}$) or IL-4 knockout (IL-$4^{-/-}$) animals after 48-h cold exposure. Quantitative PCR analysis of beige markers in sWAT (*B*) or brown markers in BAT (*C*). H&E stains of sWAT (*D*) and BAT (*E*). *F*: Immunohistochemistry for UCP1 (red stain) and perilipin (green) of sWAT isolated from IL-$4^{+/+}$ or IL-$4^{-/-}$ animals after 48-h cold exposure. Scale bars = 100 μm (*D*) and 50 μm (*E* and *F*).

removed the dox from the food and analyzed the sWAT after 7 and 12 days of VEGF-A washout (Fig. 7*A*). Dox is usually washed out within 12–16 h after its removal (21,22). The sWAT from the Tg mice looks visibly browner after 3 days of induction of VEGF-A with dox. The color of the sWAT appears paler and reaches normal after 12 days of dox washout (Fig. 7*A*). Histologically, the characteristic multilocular appearance disappears within the same time frame, as judged by H&E stains (Fig. 7*B*). These observations are further confirmed at the gene expression level (Fig. 7*C* and *D*). UCP1 and VEGF-A reach levels of controls after 7 days and in fact fall even below normal levels in the controls by day 12, likely because of a compensatory response to the previous elevation of the levels during dox exposure.

DISCUSSION

Angiogenesis is an important component of adipose tissue remodeling under both normal and pathophysiological conditions (1). Proper adipose tissue vascularization is essential to maintain normal tissue homeostasis. Improvements in adipose tissue angiogenesis offer a potential therapeutic avenue for metabolic diseases (23). Various cytokines secreted from adipocyte, such as leptin, adiponectin, hepatocyte growth factor, fibroblast growth factor, platelet-derived growth factor, transforming growth factor-β, and VEGF as well as the butyric acid derivative monobutyrin, exert established angiogenic activities in adipose tissue (2). Particularly, a host of recent studies have suggested that adipose tissue–derived VEGF, a bona fide endothelial growth factor, plays a crucial role in adipose tissue plasticity and, secondary to that, in systemic metabolism (4,5,24,25). In this study, we focused on the temporal aspects of VEGF-A action in adipocytes and the advantages this confers upon transplanting the tissue. To our surprise, local overexpression of VEGF-A in adipose tissue very rapidly triggers angiogenesis and browning of sWAT, with initial signs apparent as early as 2 days after exposure to higher levels of VEGF-A. We were particularly surprised how quickly the transformation of sWAT occurred, and this happens with VEGF-A levels well within the physiological range, because massive overexpression of VEGF-A can lead to edema formation and needs to be avoided (4). As such, VEGF-A is probably one of the most potent "beiging" factors described to date or minimally, the only one for which such a refined time course of action is being described. Our previous data (26) have shown that either cold-induced or β3-adrenergic agonist–mediated beiging of sWAT is primarily because of de novo recruitment of precursor cells. Whether a similar mechanism is in place for VEGF-A–mediated beiging is difficult to address, as two parallel inducible systems would be required to do the traditional pulse/chase experiments.

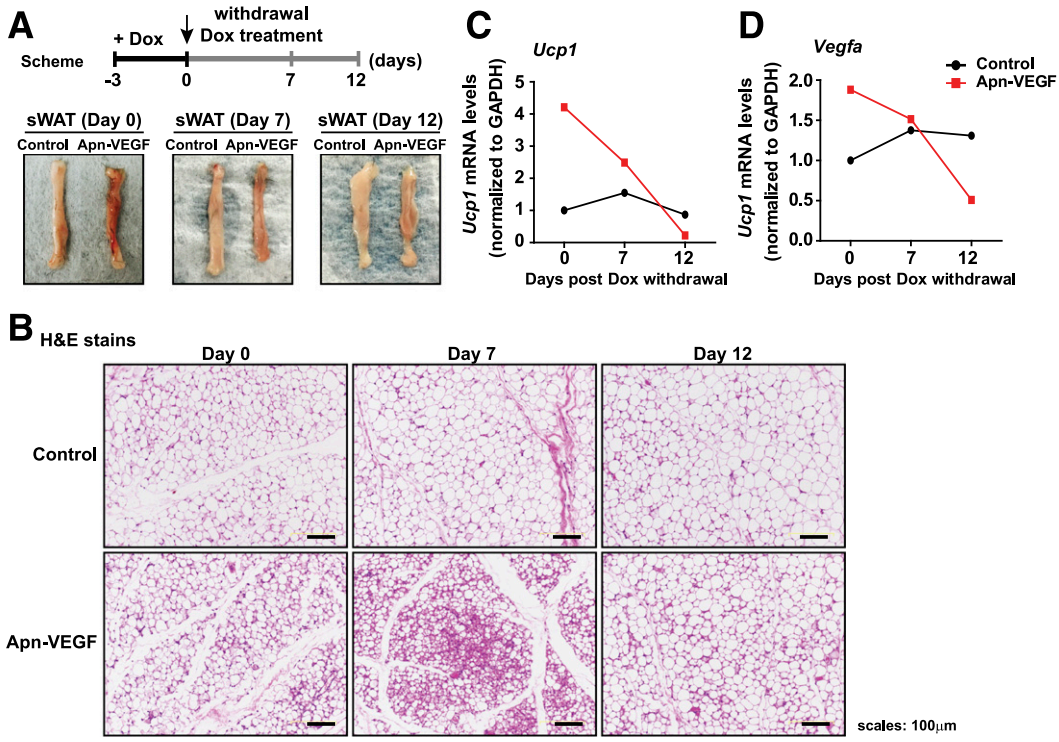

Figure 7—VEGF-A washout causes conversion from beige to white adipocytes. *A*: Schematic diagram of the experiment and images of sWAT at the different time points. *B*: H&E stain of fat pads from control and Tg mice harvested at different time points of washout. Scale bars = 100 μm. Quantitative PCR analysis of UCP1 (*C*) and VEGF-A (*D*) over the course of the washout experiment.

However, because mature adipocytes do not express VEGF-A receptors, and the addition of VEGF-A in tissue culture does not cause any degree of browning (4), it seems unlikely that a simple "*trans*-differentiation" mechanism is in place despite the unexpectedly rapid kinetics observed in this study. Interesting recent data also point toward an intracrine-signaling mechanism of VEGF. VEGF can control differentiation in mesenchymal stem cells that are osteogenic precursors by acting through the activation of the transcription factors RUNX2 and peroxisome proliferator–activated receptor γ2 as well as through interactions with the nuclear envelope proteins lamin A/C. This intracrine signaling mechanism is distinct from the role of secreted VEGF-A and its receptors (27). We cannot exclude that such a mechanism is in place in this study as well. What is, however, quite clear is that the expansion of the vasculature precedes the appearance of UCP1-positive cells, highlighting an interesting temporal relationship between the two processes. Future experiments will have to highlight whether the mere expansion of the vasculature is sufficient for the process of beiging or whether there is an additional VEGF-A–dependent component to the process. Also quite apparent but less surprising is the observation that the beige adipocytes induced by VEGF-A require the continued presence of VEGF-A. Loss of ectopic expression of VEGF-A results in the disappearance of the beige adipocytes within 7 to 12 days, presumably through conversion to white adipocytes.

We chose adipose tissue transplantation as a model system to probe for adipose tissue health and survival benefits induced by VEGF. Fat implantation is a common technique for the repair of tissue defects in plastic and reconstructive surgery. However, the survival rates of adipocytes in fat grafts are varying depending on numerous conditions during surgery (28–30). Therefore, establishment of stable and optimized conditions to sustain adipocyte health and survival is critical for a successful surgical fat implantation. In this study, we show that VEGF-overexpressing adipose tissue confers enhanced adipocyte survival with reduced chronic inflammation, leading to improvements in systemic metabolic parameters in diet-challenged obese hosts. The experiments demonstrate that the original phenotype of the adipose tissue from the donor is maintained in the host over prolonged periods and can convey significant metabolic benefits to the host. Similar results have been reported by Min et al. (31) for human beige fat transplants, commented on by Wang and Scherer (32). These authors demonstrated that they can differentiate human beige precursors in vitro into beige adipocytes. These cells can be transplanted into nude mice, in which they can positively affect systemic glucose homeostasis. The findings we report in this study with Tg VEGF-A are very much in line with the results reported by Wang and Scherer (32) and Min et al. (31), highlighting how small patches of transplanted fat can cause significant improvements in metabolic homeostasis.

Finally, we also studied this model with an eye on deeper mechanistic events leading to the beiging process. In particular, Qiu et al. (20) described an efferent beige fat

thermogenic circuit that consists of eosinophils, the type 2 cytokines IL-4/13, and alternatively activated macrophages. In this model, macrophages are recruited to cold-stressed subcutaneous adipose tissue, undergo alternative activation, and induce tyrosine hydroxylase activity along with catecholamine production, factors critical for the beiging process. We tested whether the VEGF-A–mediated beiging process has similar requirements by breeding the inducible adipocyte-specific VEGF-A system into the IL-4–null background. IL-4–null mice indeed showed a reduced propensity toward beiging and browning in the cold. However, the VEGF-A–mediated beiging was unaffected by the absence of IL-4. This is the first example in which the beiging process has been studied outside the scope of cold exposure with respect to the postulated involvement of macrophages and the associated catecholamine production. During the time course, we indeed observe a transient infiltration of macrophages after 24 h, which subsequently rapidly dissipates. Altogether, this hints at important differences between classic cold-mediated effects and at least VEGF-A–induced beiging. Similar results held true for VEGF-A effects in adiponectin null mice.

As additional beiging factors are being described in the literature, it will be interesting to see what commonalities and distinctions can be found regarding the mechanisms driving the beiging process among the different factors and the cold-induced beiging process.

Acknowledgments. The authors thank the University of Texas Southwestern Medical Center Molecular Pathology Core for help with histology and the Metabolic Phenotyping Core Facility for help with the phenotyping.

Funding. This work was supported by the National Institutes of Health (R01-DK55758, R01-DK099110, and P01-DK088761) as well as a grant from the Cancer Prevention and Research Institute of Texas (CPRIT RP140412 to P.E.S.). This work was also supported by a grant from the Korea Health Technology R&D Project through the Korea Health Industry Development Institute funded by the Ministry of Health & Welfare, Republic of Korea (HI14C1277) and a grant from the Basic Science Research Program through the National Research Foundation of Korea funded by the Ministry of Education (NRF-2014R1A1A2054914 to J.P.). M.K. was supported by the Priority Research Centers Program through the National Research Foundation of Korea funded by the Ministry of Education, Science and Technology (2010-0020224). K.S. was supported by a pilot award from the Center for Clinical and Translational Sciences at The University of Texas Health Science Center at Houston (UL1-TR-000371).

Duality of Interest. No potential conflicts of interest relevant to this article were reported.

Author Contributions. J.P., M.K., K.S., Y.A.A., and X.G. contributed to the data collection and analysis. J.P., M.K., K.S., and P.E.S. contributed to the study conception and design and writing of the manuscript. P.E.S. is the guarantor of this work and, as such, had full access to all the data in the study and takes responsibility for the integrity of the data and the accuracy of the data analysis.

Prior Presentation. Parts of this study were presented in poster form and as a portion of the keynote lecture at the Keystone Symposia on Diabetes, joint with Obesity and Adipose Tissue Biology, Keystone, CO, 22–26 January 2017.

References

1. Sun K, Kusminski CM, Scherer PE. Adipose tissue remodeling and obesity. J Clin Invest 2011;121:2094–2101
2. Cao Y. Angiogenesis and vascular functions in modulation of obesity, adipose metabolism, and insulin sensitivity. Cell Metab 2013;18:478–489
3. Olsson AK, Dimberg A, Kreuger J, Claesson-Welsh L. VEGF receptor signalling - in control of vascular function. Nat Rev Mol Cell Biol 2006;7:359–371
4. Sun K, Wernstedt Asterholm I, Kusminski CM, et al. Dichotomous effects of VEGF-A on adipose tissue dysfunction. Proc Natl Acad Sci U S A 2012;109:5874–5879
5. Sun K, Kusminski CM, Luby-Phelps K, et al. Brown adipose tissue derived VEGF-A modulates cold tolerance and energy expenditure. Mol Metab 2014;3:474–483
6. Bauer-Kreisel P, Goepferich A, Blunk T. Cell-delivery therapeutics for adipose tissue regeneration. Adv Drug Deliv Rev 2010;62:798–813
7. Sommer B, Sattler G. Current concepts of fat graft survival: histology of aspirated adipose tissue and review of the literature. Dermatol Surg 2000;26:1159–1166
8. Topcu A, Aydin OE, Ünlü M, Barutcu A, Atabey A. Increasing the viability of fat grafts by vascular endothelial growth factor. Arch Facial Plast Surg 2012;14:270–276
9. Chung CW, Marra KG, Li H, et al. VEGF microsphere technology to enhance vascularization in fat grafting. Ann Plast Surg 2012;69:213–219
10. Park J, Euhus DM, Scherer PE. Paracrine and endocrine effects of adipose tissue on cancer development and progression. Endocr Rev 2011;32:550–570
11. Mojallal A, Lequeux C, Shipkov C, et al. Stem cells, mature adipocytes, and extracellular scaffold: what does each contribute to fat graft survival? Aesthetic Plast Surg 2011;35:1061–1072
12. Yamaguchi M, Matsumoto F, Bujo H, et al. Revascularization determines volume retention and gene expression by fat grafts in mice. Exp Biol Med (Maywood) 2005;230:742–748
13. Nishimura T, Hashimoto H, Nakanishi I, Furukawa M. Microvascular angiogenesis and apoptosis in the survival of free fat grafts. Laryngoscope 2000;110:1333–1338
14. Wu Y, Wu T, Wu J, et al. Chronic inflammation exacerbates glucose metabolism disorders in C57BL/6J mice fed with high-fat diet. J Endocrinol 2013;219:195–204
15. Smorlesi A, Frontini A, Giordano A, Cinti S. The adipose organ: white-brown adipocyte plasticity and metabolic inflammation. Obes Rev 2012;13(Suppl. 2):83–96
16. Wu J, Boström P, Sparks LM, et al. Beige adipocytes are a distinct type of thermogenic fat cell in mouse and human. Cell 2012;150:366–376
17. Sun K, Park J, Gupta OT, et al. Endotrophin triggers adipose tissue fibrosis and metabolic dysfunction. Nat Commun 2014;5:3485
18. Combs TP, Pajvani UB, Berg AH, et al. A transgenic mouse with a deletion in the collagenous domain of adiponectin displays elevated circulating adiponectin and improved insulin sensitivity. Endocrinology 2004;145:367–383
19. Asterholm IW, Scherer PE. Enhanced metabolic flexibility associated with elevated adiponectin levels. Am J Pathol 2010;176:1364–1376
20. Qiu Y, Nguyen KD, Odegaard JI, et al. Eosinophils and type 2 cytokine signaling in macrophages orchestrate development of functional beige fat. Cell 2014;157:1292–1308
21. Gschwend MH, Martin W, Erenmemişoğlu A, et al. Pharmacokinetics and bioequivalence study of doxycycline capsules in healthy male subjects. Arzneimittelforschung 2007;57:347–351
22. Ye R, Wang QA, Tao C, et al. Impact of tamoxifen on adipocyte lineage tracing: Inducer of adipogenesis and prolonged nuclear translocation of Cre recombinase. Mol Metab 2015;4:771–778
23. Cao Y. Adipose tissue angiogenesis as a therapeutic target for obesity and metabolic diseases. Nat Rev Drug Discov 2010;9:107–115
24. Elias I, Franckhauser S, Ferré T, et al. Adipose tissue overexpression of vascular endothelial growth factor protects against diet-induced obesity and insulin resistance. Diabetes 2012;61:1801–1813
25. Honek J, Seki T, Iwamoto H, et al. Modulation of age-related insulin sensitivity by VEGF-dependent vascular plasticity in adipose tissues. Proc Natl Acad Sci U S A 2014;111:14906–14911
26. Wang QA, Tao C, Gupta RK, Scherer PE. Tracking adipogenesis during white adipose tissue development, expansion and regeneration. Nat Med 2013;19:1338–1344

27. Liu Y, Berendsen AD, Jia S, et al. Intracellular VEGF regulates the balance between osteoblast and adipocyte differentiation. J Clin Invest 2012;122:3101–3113
28. Moseley TA, Zhu M, Hedrick MH. Adipose-derived stem and progenitor cells as fillers in plastic and reconstructive surgery. Plast Reconstr Surg 2006;118 (Suppl.):121S–128S
29. Guerrerosantos J. Frontalis musculocutaneous island flap for coverage of forehead defect. Plast Reconstr Surg 2000;105:18–22
30. Guerrerosantos J. Long-term outcome of autologous fat transplantation in aesthetic facial recontouring: sixteen years of experience with 1936 cases. Clin Plast Surg 2000;27:515–543
31. Min SY, Kady J, Nam M, et al. Human 'brite/beige' adipocytes develop from capillary networks, and their implantation improves metabolic homeostasis in mice. Nat Med 2016;22:312–318
32. Wang QA, Scherer PE. Human beige adipocytes: epiphenomenon or drivers of metabolic improvements? Trends Endocrinol Metab 2016;27:244–246